Electronic Supplementary Material (ESI) for Physical Chemistry Chemical Physics.

Electronic Supplementary Information

Solubilization and Coordination of the $HgCl_2$ Molecule in Water, Methanol, Acetone, and Acetonitrile: an X-ray Absorption Investigation

Matteo Busato,*[,a] Giuseppe Fazio,[a] Francesco Tavani,[a] Simone Pollastri,[b] and Paola D'Angelo*[,a]

[a]*Department of Chemistry, University of Rome "La Sapienza", P.le A. Moro 5, 00185, Rome, Italy*
[b]*Elettra-Sincrotrone Trieste S.C.p.A., s.s. 14, km 163.5, I-34149, Basovizza, Trieste, , Italy*

*Corresponding authors
E-mail:
matteo.busato@uniroma1.it
p.dangelo@uniroma1.it

1. EXAFS data analysis: three body distributions

In the analysis of the EXAFS part of the absorption spectra collected on the $HgCl_2$ crystal and on the 0.1 M $HgCl_2$ solutions in water, methanol (MeOH), acetone (Act), and acetonitrile (AN), the Cl-Hg-Cl contribution has been also considered. In the GNXAS formalism, for a three body distribution the two shortest distances r_1 and r_2 within the φ angle in between are considered.[1,2] Since these distances and angle are correlated, a covariance matrix containing bond and angle variances as well as bond-angle correlations is defined as follows:

$$\begin{pmatrix} \sigma_{r_1}^2 & \rho_{r_1 r_2}^2 & \rho_{r_1 \varphi}^2 \\ - & \sigma_{r_2}^2 & \rho_{r_2 \varphi}^2 \\ - & - & \sigma_{\varphi}^2 \end{pmatrix}$$

where the ρ_{ij} terms are expressed as $\rho_{ij} = \sigma_{ij}^2 / \sqrt{\sigma_i^2 \sigma_j^2}$. In this way, ρ_{ij} is dimensionless and defined in the $-1 \leq \rho_{ij} \leq 1$ range. For $\rho_{ij} = 0$, bonds (or angles) vibrate independently, while for $\rho_{ij} = \pm 1$ there is full correlation between the parameters, which both expand or contract at the same time for +1, while one expands the other contracts in case of -1. Note that in case of the Cl-Hg-Cl distribution the terms for r_1 and r_2 are identical, as there is only one Hg-Cl path related to the first shell chlorine atoms.

Table S1. Optimized parameters for the three body Cl-Hg-Cl distribution as determined from the EXAFS data analysis of the Hg L_3-edge absorption spectra of crystalline $HgCl_2$ and of the $HgCl_2$ 0.1 M solutions in water, MeOH, Act, and AN. The bond angle values are reported with the standard deviation σ_φ in parenthesis, while the ρ_{rr} *and* $\rho_{r\varphi}$ terms are referred to the bond-bond and bond-angles correlations, respectively.

	Cl-Hg-Cl angle (°)	ρ_{rr}	$\rho_{r\varphi}$
$HgCl_2$	180(5)	0.4	0.2
$HgCl_2$ in H_2O	180(4)	0.5	0.3
$HgCl_2$ in MeOH	180(4)	0.5	0.3
$HgCl_2$ in Act	180(4)	0.4	0.2
$HgCl_2$ in AN	180(4)	0.2	0.1

Table S2. Optimized non-structural parameters for the ionization energy E_0 and for the amplitude reduction factor S_0^2 as determined from the EXAFS data analysis of the Hg L_3-edge absorption spectra of crystalline $HgCl_2$ and of the $HgCl_2$ 0.1 M solutions in water, MeOH, Act, and AN. The E_0 is given as difference with respect to the inflection point of the experimental spectrum after the pre-edge peak.

	E_0 - E_t (eV)	S_0^2
$HgCl_2$	2.1	0.96
$HgCl_2$ in H_2O	0.3	0.95
$HgCl_2$ in MeOH	0.2	0.90
$HgCl_2$ in Act	1.2	1.00
$HgCl_2$ in AN	0.0	0.96

Table S3. Double-electron excitation edge parameters as determined from the EXAFS data analysis of the Hg L_3-edge absorption spectra of crystalline $HgCl_2$ and of the $HgCl_2$ 0.1 M solutions in water, MeOH, Act, and AN, compared with the Z + 1 predictions.[†]

		E_d - E_t (eV)	H	ΔE (eV)	E_{Z+1} (eV)
$HgCl_2$	$2p_{3/2}5p_{3/2}$	70	0.09	7	73
	$2p_{3/2}5p_{1/2}$	-	-	-	95
$HgCl_2$ in H_2O	$2p_{3/2}5p_{3/2}$	62	0.13	14	73
	$2p_{3/2}5p_{1/2}$	94	0.02	7	95
$HgCl_2$ in MeOH	$2p_{3/2}5p_{3/2}$	61	0.16	14	73
	$2p_{3/2}5p_{1/2}$	92	0.04	13	95
$HgCl_2$ in Act	$2p_{3/2}5p_{3/2}$	67	0.04	3	73
	$2p_{3/2}5p_{1/2}$	-	-	-	-
$HgCl_2$ in AN	$2p_{3/2}5p_{3/2}$	64	0.24	15	73
	$2p_{3/2}5p_{1/2}$	97	0.02	7	95

[†]The double-excitation energy onset E_d is measured from the correspondent inflection point of the experimental spectrum E_t. The absorption discontinuities H are given in jump units. ΔE are the energies of the double-electron channel width.

Table S4. Best-fit structural parameters for the Hg-Cl and Hg-O SS paths obtained from the analysis of the Hg L_3-edge EXAFS spectrum collected on the 0.1 M $HgCl_2$ solution in water, carried out with the model with three water molecules around the $HgCl_2$ unit.†

	N	*R* (Å)	σ^2 (Å^2)	*β*
Hg-Cl	2.0	2.32(2)	0.003(2)	0.3(1)
Hg-O	3.0	2.78(4)	0.075(4)	0.8(2)

†*N* is the coordination number, *R* the average distance, σ^2 the Debye-Waller factor, and *β* the asymmetry index.

Table S5. Structural and non-structural parameters obtained from the XANES analysis of the Hg L_3-edge experimental spectrum collected on the 0.1 M $HgCl_2$ aqueous solution for a $HgCl_2$ molecule with a 170° and 175° Cl-Hg-Cl angle, plus three water molecules. $R_{Hg\text{-}Cl}$ and $R_{Hg\text{-}O}$ are respectively the Hg-Cl and Hg-O distances, E_0 is the threshold energy, E_F the Fermi energy, E_S and A_S the plasmon energy onset and amplitude, and Γ_{exp} the experimental resolution.

Cl-Hg-Cl angle	$R_{Hg\text{-}Cl}$ (Å)	$R_{Hg\text{-}O}$ (Å)	E_0 (eV)	E_F (eV)	E_S (eV)	A_S	Γ_{exp} (eV)
175°	2.21(8)	2.75(8)	0.5	-3.8	11.2	11.4	3.6
170°	2.21(8)	2.75(8)	0.5	-3.9	11.1	12.4	3.5

Table S6. Structural and non-structural parameters obtained from the XANES analysis of the Hg L_3-edge experimental spectrum collected on the 0.1 M $HgCl_2$ solution in Act for the structure with three solvent molecules. $R_{Hg\text{-}Cl}$ and $R_{Hg\text{-}O}$ are respectively the Hg-Cl and Hg-O distances, E_0 is the threshold energy, E_F the Fermi energy, E_S and A_S the plasmon energy onset and amplitude, and Γ_{exp} the experimental resolution.

$R_{Hg\text{-}Cl}$ (Å)	$R_{Hg\text{-}O}$ (Å)	E_0 (eV)	E_F (eV)	E_S (eV)	A_S	Γ_{exp} (eV)
2.24(8)	2.68(8)	-1.26	-4.7	3.6	13.5	3.1

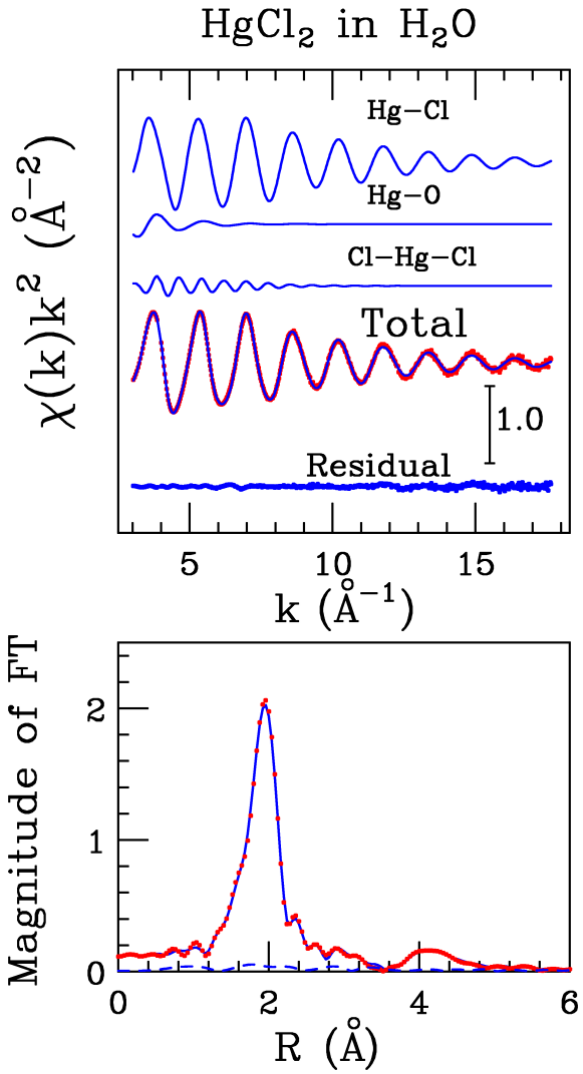

Figure S1. Upper panel: analysis of the Hg L_3-edge EXAFS spectrum collected on the 0.1 M $HgCl_2$ solution in water, carried out with the model with three water molecules around the $HgCl_2$ unit. From the top the best-fit theoretical signals Hg-Cl accounting for the two first shell chlorine atoms, Hg-O accounting for the three oxygen atoms of the water molecules, and for the three-body Cl-Hg-Cl distribution are shown, together with the total theoretical spectrum (blue line) compared with the experimental one (red dots) and the resulting residuals (blue dots). Lower panel: non-phase shift corrected Fourier Transforms of the best-fit EXAFS theoretical signal (blue line), of the experimental data (red dots) and of the residual curve (blue-dashed line). The FT has been calculated in the 3.0 – 16.7 $Å^{-1}$ *k*-range.

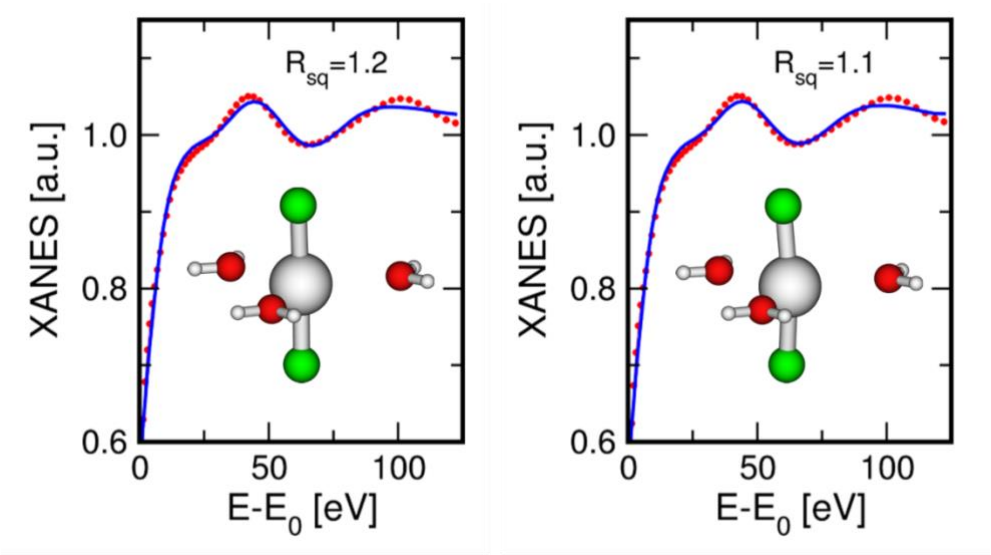

Figure S2. Comparison between the Hg L_3-edge XANES experimental spectra collected on the 0.1 M $HgCl_2$ aqueous solution (red dots) with the theoretical signals (blue lines) calculated for a $HgCl_2$ molecule with a 175° (left panel) and 170° (right panel) Cl-Hg-Cl angle, plus three water molecules. The obtained residual function R_{sq} and the optimized clusters are shown as insets.

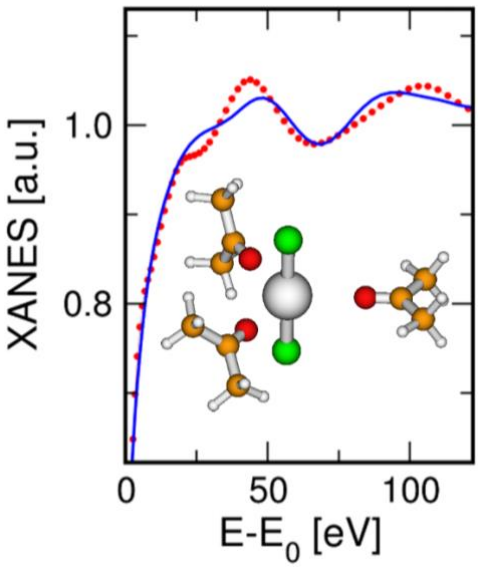

Figure S3. Comparison between the Hg L_3-edge XANES experimental spectrum collected on the 0.1 M $HgCl_2$ Act solution (red dots) compared with the theoretical signal (blue line) calculated with a starting structure where three Act molecules coordinate the $HgCl_2$ unit in a trigonal bipyramidal structure. The optimized cluster is shown as inset.

References

1 A. Filipponi and A. Di Cicco, X-ray-absorption spectroscopy and n-body distribution functions in condensed matter. I. Theory, *Phys. Rev. B*, 1995, **52**, 15122–15134.

2 A. Filipponi and A. Di Cicco, X-ray-absorption spectroscopy and n-body distribution functions in condensed matter. II. Data analysis and applications, *Phys. Rev. B*, 1995, **52**, 15135–15149.